Chapter 5

A numerical solution of a non-classical Stefan problem with space-dependent thermal conductivity, variable latent heat and Robin boundary condition

5.1 Introduction

A one-phase Stefan problem occurs in the phase change process that involves a diffusion equation and a moving phase front (moving boundary). In this problem, we require to investigate the temperature distribution in the time-dependent domain and the movement of the moving boundary. Classical Stefan problems arise in many daily life problems such as the melting of materials, freezing of liquid, food preservation, reintegration of metals, oxygen diffusion process, etc. The detailed studies of the classical Stefan problems were discussed in [3, 99, 100]. In the last few decades, studies of Stefan problems have gained a great attention due to their non-linear nature, presence of the time-dependent domain, and wide range of applications in engineering, biological and industrial processes [178, 179, 180, 145, 147, 181], such as melting and freezing processes, molecular diffusion process, sedimentation process, photovoltaic electricity systems, vanishing and spreading of the species, drug-release process, tumor growth and crystal growth. The applications of Stefan problem can also be found in the thermal energy storage devices. At present, thermal energy

storage has become an exciting and valuable area of renewable energy, and some recent developments in this area can be seen in [182, 183, 184].

Nowadays, apart from the classical Stefan problems, some mathematical models of non-classical Stefan problems have been formulated, including variable thermal coefficients or/and variable latent heat. Ceretani et al. [84] have taken temperature-dependent thermal coefficients for a phase change problem and presented an analytical solution to the problem. Voller and Falcini [81] have developed two closed analytical solutions to the one-phase one-dimensional Stefan problem for two different types of space-dependent thermal diffusivity. A Stefan problem with variable latent heat was discussed by Voller et al. [78], they presented an analytical solution to this problem. A time-fractional Stefan problem with variable latent heat has also been discussed by Rajeev and Kushwaha [134]. Moreover, in past decades, the non-classical heat transfer problems for a semi-infinite length material have been deliberated in [185, 186, 187]. A Stefan problem governed by the non-classical heat equation with constant thermal coefficients was discussed by Briozzo and Tarzia [80]. A phase change problem of a non-classical heat equation with the temperature-dependent thermal coefficients in a semi-infinite domain was discussed in [165]. Zhou et al. [82] presented a phase change problem including space-dependent latent heat in their study and established an analytical solution to the problem. In 2019, Singh et al. [85] presented a Stefan problem including the moving phase change material (MPCM) and variable thermal coefficients. Font [46] has discussed the space-dependent thermal conductivity in a one-phase Stefan problem and the approximate solution to the problem. Kumar and Rajeev [69] also considered space-dependent thermal conductivity in a Stefan problem with a MPCM, and they discussed a numerical solution to the problem. Motivated by the above research articles, a non-classical Stefan problem (moving boundary problem) is considered

with the following space-dependent thermal conductivity:

$$\kappa(z,\tau) = \kappa_0\Big(1 + \delta\frac{z}{S(\tau)}\Big), \tag{5.1}$$

where κ_0 is the constant thermal conductivity, z is the space variable, τ is the time, $S(\tau)$ is the melting front, δ is the positive constant.

From the literature [188, 189], it is found that the analytical solutions to non-linear partial differential equations (PDE) are limited, and this is the main reason for the researchers to choose appropriate numerical schemes/numerical simulations. Some recent papers on numerical techniques or numerical simulations for solving various PDEs are reported in [190, 191, 192, 193, 194]. The exact solutions to the Stefan problems are also not easy to establish in the case of variable thermal coefficients due to the non-linearity of the heat equation in the time-dependent domain. Therefore, several numerical methods have been developed to solve the Stefan problems [68, 120]. Besides these numerical techniques, operational matrix methods attract many researchers to find the approximate solution to the Stefan problem because of its exponential rate of convergence. In 2020, Kumar and Rajeev [70] presented the solution to a Stefan problem with the aid of the operational matrix method based on shifted Chebyshev polynomials. The operational matrix method based on shifted Legendre polynomials has been applied by Singh et al. [86] to solve a Stefan problem including MPCM and variable thermal coefficients. In this chapter, an operational matrix method is used which is based on transformed Genocchi polynomials and the collocation scheme. Some properties of Genocchi numbers and Genocchi polynomials can be seen in [195, 196, 197]. The operational matrix based on Genocchi polynomials for the interval [0, 1] has been discussed in [198] and applied to the delay differential equations. In [199], a numerical solution of the non-linear fractional

differential equation with the help of new operational matrix based on Genocchi polynomials has also been discussed in the literature.

5.2 Preliminaries

Properties of Genocchi numbers and Genocchi polynomials have been widely discussed by many researchers in the different mathematical branches; for example elementary number theory, differential topology, homology number theory, etc. Usually, the Genocchi number G_m is defined with the aid of the exponential generating functions [195, 197, 196] as given below:

$$\frac{2y}{e^y+1} = \sum_{m=0}^{\infty} G_m \frac{y^m}{m!}, \ (|y| < \pi). \tag{5.2}$$

With the help of the exponential generating functions, the classical Genocchi polynomials [195, 199] $G_m(z)$ is stated as

$$\frac{2ye^{zy}}{e^y+1} = \sum_{m=0}^{\infty} G_m(z) \frac{y^m}{m!}, \ (|y| < \pi). \tag{5.3}$$

The Genocchi polynomial $G_m(z)$ of degree $m-1$ on the interval $[0,1]$ is given by

$$G_m(z) = \sum_{k=0}^{m} {}^mC_k G_k z^{m-k}. \tag{5.4}$$

where G_k is the Genocchi number.

In order to use these polynomials in the interval $[0, \lambda]$, the transformation $z = \frac{x}{\lambda}$ is introduced and the transformed Genocchi polynomials $G^*_m(x)$ becomes

$$G^*_m(x) = \sum_{k=0}^{m} {}^mC_k G_k \Big(\frac{x}{\lambda}\Big)^{m-k}. \tag{5.5}$$

The first few transformed Genocchi polynomials defined on the interval $[0, \lambda]$ are given below:

$$\begin{aligned}
G^*_1(x) &= 1,\\
G^*_2(x) &= 2\Big(\frac{x}{\lambda}\Big) - 1,\\
G^*_3(x) &= 3\Big(\frac{x}{\lambda}\Big)^2 - 3\Big(\frac{x}{\lambda}\Big),\\
G^*_4(x) &= 4\Big(\frac{x}{\lambda}\Big)^3 - 6\Big(\frac{x}{\lambda}\Big)^2 + 1,\\
G^*_5(x) &= 5\Big(\frac{x}{\lambda}\Big)^4 - 10\Big(\frac{x}{\lambda}\Big)^3 + 5\Big(\frac{x}{\lambda}\Big).
\end{aligned}$$

The derivative of (5.5) with respect to x gives us

$$\frac{dG^*_m}{dx} = \frac{mG^*_{m-1}}{\lambda}, \quad m \geqslant 1. \tag{5.6}$$

Now, the vector form of transformed Genocchi polynomials $\mathbf{G}^*(x)$ is taken as

$$\mathbf{G}^*(x) = [G^*_1(x), G^*_2(x), \cdots, G^*_M(x)].$$

According to Isah and Phang [198], the k^{th} derivative of vector $\mathbf{G}^*(x)$ is given by

$$\mathbf{G}^{*(k)}(x) = \mathbf{G}^*(x)(\mathbf{D}^T)^k, \tag{5.7}$$

where

$$\mathbf{D} = \frac{1}{\lambda}\begin{bmatrix} 0 & 0 & 0 & 0 & \dots & 0 & 0 & 0 \\ 2 & 0 & 0 & 0 & \dots & 0 & 0 & 0 \\ 0 & 3 & 0 & 0 & \dots & 0 & 0 & 0 \\ 0 & 0 & 4 & 0 & \dots & 0 & 0 & 0 \\ \vdots & \vdots & \vdots & \vdots & \ddots & \vdots & \vdots & \vdots \\ 0 & 0 & 0 & 0 & \dots & M-1 & 0 & 0 \\ 0 & 0 & 0 & 0 & \dots & 0 & M & 0 \end{bmatrix} \quad \textit{and} \quad [\mathbf{G}^{*(k)}(x)]^T = \begin{bmatrix} G_1^{*(k)}(x) \\ G_2^{*(k)}(x) \\ G_3^{*(k)}(x) \\ G_4^{*(k)}(x) \\ \vdots \\ {G^*_{M-1}}^{(k)}(x) \\ {G^*_M}^{(k)}(x) \end{bmatrix}.$$

Now, let us assume that a square integrable function $h(x)$ defined on $[0, \lambda]$ can be expressed as the linear sum of first M terms of the transformed Genocchi polynomial $G^*(x)$. Thus, the following can be written as

$$h(x) = \sum_{m=1}^{M} C_m G_m^*(x) = \mathbf{G}^*(x)\mathbf{C}, \tag{5.8}$$

where the constant vector $\mathbf{C}$ is given by $\mathbf{C}^T = [C_1, C_2, \cdots, C_M]$ and the k^{th} derivative of $h(x)$ is expressed as

$$h^{(k)}(x) = \mathbf{G}^*(x)(\mathbf{D}^T)^k\mathbf{C}. \tag{5.9}$$

5.3 Mathematical formulation and its solution

5.3.1 Mathematical model

Here, a non-classical one-phase Stefan problem ([165, 82, 69]) is considered in a semi-infinite range in one-dimensional corresponding to the melting process with space-dependent thermal conductivity, variable latent heat and Robin boundary condition at the fixed boundary $z = 0$. The mathematical formulation of the problem is given below:

$$\rho c \frac{\partial U}{\partial \tau} = \frac{\partial}{\partial z}\left(\kappa(z,\tau)\frac{\partial U}{\partial z}\right) + \frac{\zeta_0}{\sqrt{\tau}}\frac{\partial U}{\partial z}(0,\tau),$$

$$0 < z < S(\tau), \quad \tau > 0, \tag{5.10}$$

$$\kappa(0,\tau)\frac{\partial U}{\partial z}(0,\tau) = \frac{h}{\sqrt{\tau}}(U(0,\tau) - U_\infty \tau^{\alpha/2}), \tag{5.11}$$

$$U(S(\tau),\tau) = 0, \tag{5.12}$$

$$\kappa(S(\tau),\tau)\frac{\partial U}{\partial z}(S(\tau),\tau) = -\gamma S^\alpha(\tau)\frac{dS}{d\tau}, \tag{5.13}$$

$$S(0) = 0, \tag{5.14}$$

where U is the temperature distribution in $0 < z < S(\tau)$, κ is the space-dependent thermal conductivity as given in Eq. (5.1), τ is the time, $U_\infty \tau^{\alpha/2}$ characterizes the surrounding temperature at the fixed face $z = 0$ with the positive constant α, h represents the convective heat transfer coefficient, c is the specific heat capacity, ρ is the density of the material, ζ_0 is the given positive constant and the dimension of ζ_0 is given by $MK^{-1}T^{-5/2}$. $\gamma z^\alpha(\tau)$ is the space dependent latent heat with γ as a real constant.

5.3.2 Similarity transform

In this section, first, the following similarity variables are introduced to transform the Eqs. (5.10)-(5.14) into a system of ordinary differential equations:

$$U(z,\tau) = U_\infty \tau^{\alpha/2}\Psi(\eta), \quad \eta = \frac{z}{2\sqrt{\nu\tau}}, \tag{5.15}$$

and let us take the melting front as

$$S(\tau) = 2\xi\sqrt{\nu\tau}, \tag{5.16}$$

where ν is the thermal diffusivity given by $\nu = \frac{\kappa_0}{\rho c}$ and ξ is a positive constant. From Eq.(5.15) and Eq. (5.16), the system (5.10)-(5.14) reduces to

$$\frac{d}{d\eta}\left(\left(1+\delta\frac{\eta}{\xi}\right)\frac{d\Psi}{d\eta}\right) + 2\eta\frac{d\Psi}{d\eta} + 2\zeta\frac{d\Psi}{d\eta}(0) - 2\alpha\Psi(\eta) = 0, \quad 0 < \eta < \xi, \tag{5.17}$$

$$\frac{d\Psi}{d\eta}(0) = 2Bi(\Psi(0) - 1), \tag{5.18}$$

$$\Psi(\xi) = 0, \tag{5.19}$$

$$\frac{d\Psi}{d\eta}(\xi) = -\frac{2^{\alpha+1}\xi^{\alpha+1}}{Ste(1+\delta)}, \tag{5.20}$$

where $\zeta = \frac{\zeta_0}{\rho c\sqrt{\nu}}$ is a dimensionless number, generalized Biot number $Bi = \frac{h\sqrt{\nu}}{\kappa_0}$ and the generalized Stefan number $Ste = \frac{\kappa_0 U_\infty}{\nu^{\alpha/2+1}\gamma}$.

5.3.3 Operational matrix method with collocation scheme

This section consists the solution of the problem (5.17)-(5.20) by using the operational matrix of differentiation based on the transformed Genocchi polynomials.

First, the function $\Psi(\eta)$ is approximated as

$$\Psi(\eta) = \theta(\eta)\mathbf{C}, \tag{5.21}$$

where the transformed Genocchi vector $\theta(\eta)$ and coefficient vector $\mathbf{C}$ are given by $\theta(\eta)$=$[G_1^*(\eta), G_2^*(\eta), \cdots, G_M^*(\eta)]$ and $\mathbf{C}^T$=$[C_1, C_2, \cdots, C_M]$, respectively.
Hence the Eq. (5.9) gives

$$\frac{d\Psi}{d\eta} = \theta(\eta)\mathbf{D}^T\mathbf{C} \quad and \quad \frac{d^2\Psi}{d\eta^2} = \theta(\eta)(\mathbf{D}^T)^2\mathbf{C}. \tag{5.22}$$

Now, after substituting the Eqs. (5.21) and (5.22) in the Eq. (5.17), the following residual corresponding to the Eq. (5.17) can be obtained:

$$\begin{aligned} R_M(\eta) = &\left(1 + \delta\frac{\eta}{\xi}\right)\theta(\eta)(\mathbf{D}^T)^2\mathbf{C} + \left(2\eta + \frac{\delta}{\xi}\right)\theta(\eta)\mathbf{D}^T\mathbf{C} \\ &+ 2\zeta\theta(\mathbf{0})\mathbf{D}^T\mathbf{C} - 2\alpha\theta(\eta)\mathbf{C}. \end{aligned} \tag{5.23}$$

After collocating the R_M at the collocation points $\eta_j = \frac{j}{M-2}$, where, $j = 1, 2, ..., M-2$, $(M-2)$ algebraic equations with $(M+1)$ unknowns can be found.

Next, substituting the Eqs. (5.21) and (5.22) into the Eqs. (5.18)-(5.20), we get the following three equations:

$$\theta(0)\mathbf{D}^T\mathbf{C} = 2Bi(\theta(0)\mathbf{C} - 1), \tag{5.24}$$

$$\theta(\xi)\mathbf{C} = 0, \tag{5.25}$$

$$\theta(\xi)\mathbf{D}^T\mathbf{C} = -\frac{2^{\alpha+1}\xi^{\alpha+1}}{Ste(1+\delta)}. \tag{5.26}$$

Therefore, Eq. (5.23) and Eqs. (5.24)-(5.26) generate $(M+1)$ nonlinear algebraic

equations with $(M+1)$ unknowns that can be easily solved to get the unknown constant vector $\mathbf{C}$ and ξ. Consequently, with the help of Eqs. (5.15) and (5.16), the temperature distribution $U(z,\tau)$ in the molten region $0 < z < S(\tau)$ and the location of moving melting front $S(\tau)$ can be determined.

5.4 Results and discussions

To the best of our knowledge, the analytic solution to the problem (5.10)-(5.14) has not yet been derived for non-zero δ. According to [99, 100], the analytical solution to the problem (5.10)-(5.14) for the particular case $\delta = 0$, $\alpha = 0$ and $\zeta = 0$ is given by

$$U(z,\tau) = U_\infty \frac{Bi\sqrt{\pi}\Big(erf(\xi) - erf(\frac{z}{2\sqrt{\nu\tau}})\Big)}{1 + Bi\sqrt{\pi}erf(\xi)},$$

$$0 < z < S(\tau),\ \tau > 0, \tag{5.27}$$

$$S(\tau) = 2\xi\sqrt{\nu\tau}. \tag{5.28}$$

The value of ξ can be determined by the following equation:

$$\frac{2\xi}{Ste} - \frac{2Bie^{-\xi^2}}{1 + Bi\sqrt{\pi}erf(\xi)} = 0. \tag{5.29}$$

To show the accuracy of the proposed method, the results of the operational matrix method and finite difference technique are compared with the analytic solution (5.27)-(5.29) for the particular case ($\delta = 0$, $\alpha = 0$ and $\zeta = 0$) of (5.10)-(5.14). The most common problem in looking for a numerical solution to the Stefan problem is how to discretize the moving domain that changes over time. To resolve this issue, it is necessary to define a new space variable that changes the variable domain

into a certain domain. This method is known as the front-fixing method and the transformation is called Landau-type transformation which is given below:

$$\Phi(x,\tau)=\frac{U(z,\tau)}{U_\infty \tau^{\alpha/2}},\ x=\frac{z}{S(\tau)}. \tag{5.30}$$

After using the transformation (5.30), the moving space domain converts to $0<x<1$ and Eqs. (5.10)-(5.14) becomes

$$\begin{aligned}\frac{\partial\Phi}{\partial\tau}&=\frac{\nu(1+\delta x)}{S^2(\tau)}\frac{\partial^2\Phi}{\partial x^2}+\frac{\nu\delta}{S^2(\tau)}\frac{\partial\Phi}{\partial x}+\frac{x}{S(\tau)}\frac{dS}{d\tau}\frac{\partial\Phi}{\partial x}\\&-\frac{\alpha}{2\tau}\Phi(x,\tau)+\frac{\zeta\sqrt{\nu}}{S(\tau)\sqrt{\tau}}\frac{\partial\Phi}{\partial x}(0,\tau),\end{aligned} \tag{5.31}$$

$$\frac{\partial\Phi}{\partial x}(0,\tau)=\frac{BiS(\tau)}{\sqrt{\nu\tau}}(\Phi(0,\tau)-1), \tag{5.32}$$

$$\Phi(1,\tau)=0, \tag{5.33}$$

$$\frac{\partial\Phi}{\partial x}(1,\tau)=\frac{-S^{\alpha+1}}{Ste(1+\delta)\nu^{\alpha/2+1}\tau^{\alpha/2}}\frac{dS}{d\tau}, \tag{5.34}$$

$$S(0)=0. \tag{5.35}$$

Now a forward time central space method is used to discretize the Eq. (5.31) which produces

$$\begin{aligned}\Phi_i^{n+1}=&\Phi_{i+1}^n\left(\frac{k\nu(1+\delta x_i)}{h^2S^{n2}}+\frac{k\nu\delta}{2hS^{n2}}-\frac{Ste(k\nu)^{\alpha/2+1}n^{\alpha/2}x_i}{4h^2}\right.\\&\left.\frac{(1+\delta)(\Phi_{N-2}^n-4\Phi_{N-1}^n)}{S^{n\alpha+2}}\right)+\Phi_i^n\left(1-\frac{\alpha}{2n}-\frac{2k\nu(1+\delta x_i)}{h^2S^{n2}}\right)\\&+\Phi_{i-1}^n\left(\frac{k\nu(1+\delta x_i)}{h^2S^{n2}}-\frac{k\nu\delta}{2hS^{n2}}+\frac{Ste(k\nu)^{\alpha/2+1}n^{\alpha/2}x_i}{4h^2}\right.\\&\left.\frac{(1+\delta)(\Phi_{N-2}^n-4\Phi_{N-1}^n)}{S^{n\alpha+2}}\right)+\frac{Bi\zeta(\Phi_0^n-1)}{n(1+\delta x_i)},\\&0\leqslant i\leqslant N,\ n\geqslant 0.\end{aligned} \tag{5.36}$$

For $i = 0$, the space derivative of Eq. (5.32) is approximated by central difference as given below

$$\Phi_{-1}^{n} = \Phi_{1}^{n} - \frac{2hBiS^{n}(\Phi_{0}^{n} - 1)}{\sqrt{kn\nu}}. \tag{5.37}$$

The Eq. (5.37) is used in the Eq. (5.36) to eliminate the fictitious value of Φ_{-1} from (5.36). The space derivative of Eq. (5.34) is discretized by Euler's three point backward difference and time derivative is discretized by forward difference which gives us

$$S^{n+1} = S^{n} - \frac{Ste(k\nu)^{\alpha/2+1} n^{\alpha/2}(1+\delta)(\Phi_{N-2}^{n} - 4\Phi_{N-1}^{n})}{S^{n\alpha+1}}. \tag{5.38}$$

The approximation (5.36) is consistent with $\mathcal{O}(k) + \mathcal{O}(h^2)$ and stable under the condition

$$k \leqslant \frac{h^2 Z}{2\nu}, \tag{5.39}$$

in the particular case ($\delta = 0$, $\alpha = 0$ and $\zeta = 0$, where $Z(t) = S^2(t)$) [120].

For the particular case, two tables are presented to show the accuracy of the proposed scheme. In Table 5.1, the relative errors of the temperature distribution obtained by the finite difference method (FDM) and proposed Genocchi operational matrix method (GOMM) are shown for the particular case of the problem (5.10)-(5.14) at time $\tau = 10\ s$, $\nu = 1\ m^2 s^{-1}$, $U_\infty = 10\ K$ for three different values of Bi and Ste, i.e. $((Bi = 0.5,\ Ste = 1.0),\ (Bi = 0.5, Ste = 0.5),\ (Bi = 1.0, Ste = 0.5))$. Table 5.2 presents the relative errors of the finite difference method and the Genocchi operational matrix method with the analytical solution (5.28)-(5.29) for the moving melting front at $\delta = 0$, $\alpha = 0$, $\zeta = 0$ and $\nu = 1\ m^2 s^{-1}$ for the earlier three cases

$((Bi = 0.5,\ Ste = 1.0),\ (Bi = 0.5, Ste = 0.5),\ (Bi = 1.0, Ste = 0.5))$. From Tables 5.1-5.2, it can be easily seen that the solution determined by the Genocchi operational matrix method is more accurate than the finite difference technique.

Figs. 5.1 and 5.2 are plotted to validate the correctness of the proposed numerical algorithms (GOMM) for a particular case of our model. Fig. 5.1 depicts the dependence of $\log_{10}|error|$ on the degree of Genocchi polynomials for $\Psi(\eta)$ obtained by GOMM at the parameters $\delta = 0$, $\alpha = 0$, $\zeta = 0$, $Ste = 0.5$, $Bi = 0.5$, $\nu = 1$ m^2s^{-1} and $\eta = 0.2$. In Fig. 5.2, the dependence of $\log_{10}|error|$ on the degree of Genocchi polynomials is shown at $\delta = 0$, $\alpha = 0$, $\zeta = 0$, $Ste = 0.5$, $Bi = 0.5$ and $\nu = 1$ m^2s^{-1} for the moving phase change factor (ξ). From these figures, it is numerically shown that the proposed algorithm converges rapidly when we enhance the degree of Genocchi polynomials or order of the considered operational matrix of differentiation.

Next, the considered problem (5.10)-(5.14) is solved by GOMM, and the results are presented through four figures (Figs.5.3-5.6), which show the effects of variable thermal conductivity and variable latent heat on the phase change processes. Fig. 5.3 and 5.4 are plotted at the parameters $\alpha = 1$, $\zeta = 1$, $Ste = 1.5$, $Bi = 0.75$ and $\nu = 0.5$ m^2s^{-1} for different values of δ $(\delta = 0, 1, 2, 3)$ for the temperature profile and moving phase front, respectively. From Fig. 5.3, it is observed that the temperature is maximum at $z = 0$ and continuously decreases to zero at the melting phase front. Moreover, the temperature in the molten region decreases as we increase the values of δ. Fig. 5.4 shows that the movement of melting front accelerates as we increase the parameter δ. Hence, the parameter δ affects the melting process, and the melting process enhances as the parameter δ increases. Figs. 5.5 and 5.6 are drawn at the parameters $\delta = 1$, $\zeta = 1$, $Ste = 0.5$, $Bi = 0.5$ and $\nu = 1$ m^2s^{-1} for different α $(\alpha = 0, 1, 2, 3)$ to show the effects of α on the temperature profile and the location of

moving phase front, respectively. In Fig. 5.5, the trends of the temperature profiles are reversed to the temperature profiles of Fig. 5.3, *i.e.*, the temperature in the molten region increases with the increment of α. From Fig. 5.6, it can be seen that the speed of melting front increases as we enhance the value of α. Hence, the parameter α affects the melting process, and this process becomes fast as the value of α increases.

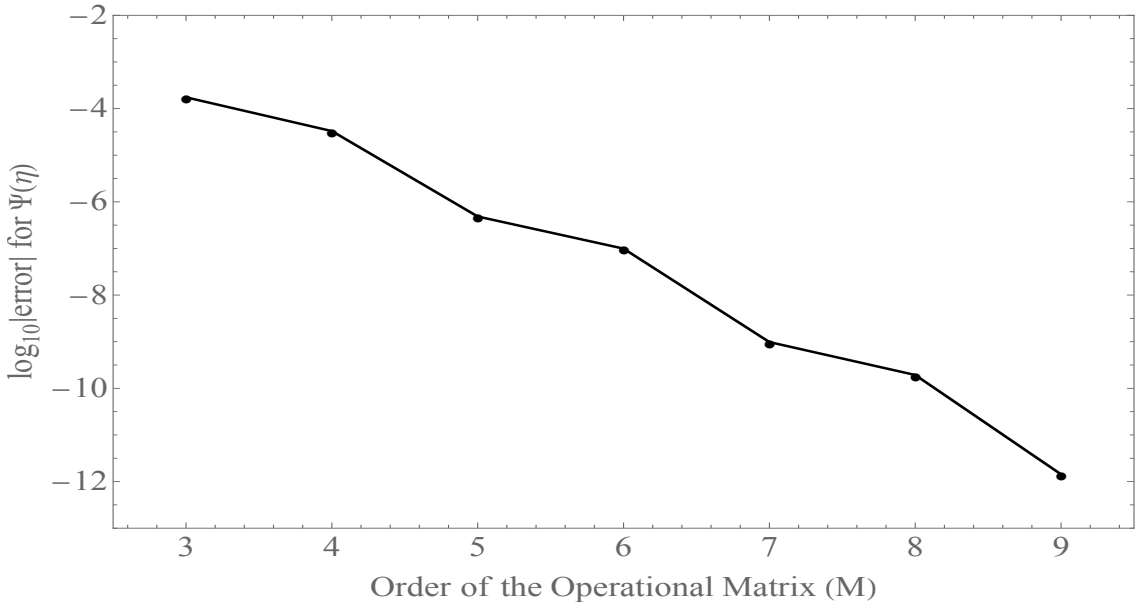

FIGURE 5.1: Convergence of approximation of temperature $\Psi(\eta)$.

TABLE 5.1: Comparison of relative error between FDM and GOMM for temperature distribution at $\alpha = 0$, $\delta = 0$, $\zeta = 0$, $\nu = 1\ m^2 s^{-1}$ and $\tau = 10\ s$ for different parameters.

S.No.	*Parameters*	x	*Relative Error*$_{FDM}$	*Relative Error*$_{GOMM}$
1		0.0	2.04141×10^{-2}	1.09658×10^{-4}
		0.1	2.05073×10^{-2}	1.19718×10^{-4}
		0.2	2.05653×10^{-2}	1.19902×10^{-4}
		0.3	2.05877×10^{-2}	1.16736×10^{-4}
		0.4	2.05745×10^{-2}	1.13819×10^{-4}
	$Bi = 0.5$	0.5	2.05256×10^{-2}	1.11873×10^{-4}
	$Ste = 1.0$	0.6	2.04411×10^{-2}	1.08785×10^{-4}
		0.7	2.03214×10^{-2}	9.96417×10^{-5}
		0.8	2.01667×10^{-2}	7.67576×10^{-5}
		0.9	1.99777×10^{-2}	2.97005×10^{-5}
		1.0	0.000000	0.000000
2		0.0	6.06276×10^{-2}	1.65683×10^{-5}
		0.1	6.07349×10^{-2}	1.78551×10^{-5}
		0.2	6.08037×10^{-2}	1.78441×10^{-5}
		0.3	6.08339×10^{-2}	1.78388×10^{-5}
		0.4	6.08255×10^{-2}	1.69605×10^{-5}
	$Bi = 0.5$	0.5	6.07784×10^{-2}	1.66554×10^{-5}
	$Ste = 0.5$	0.6	6.06928×10^{-2}	1.61912×10^{-5}
		0.7	6.05686×10^{-2}	1.49108×10^{-5}
		0.8	6.04061×10^{-2}	1.17830×10^{-5}
		0.9	6.02056×10^{-2}	5.40268×10^{-6}
		1.0	0.000000	0.000000
3		0.0	1.53753×10^{-2}	4.92444×10^{-5}
		0.1	1.54380×10^{-2}	5.50575×10^{-5}
		0.2	1.54798×10^{-2}	5.51639×10^{-5}
		0.3	1.55003×10^{-2}	5.33326×10^{-5}
		0.4	1.54996×10^{-2}	5.16465×10^{-5}
	$Bi = 1.0$	0.5	1.54775×10^{-2}	5.05203×10^{-5}
	$Ste = 0.5$	0.6	1.54342×10^{-2}	4.87315×10^{-5}
		0.7	1.53697×10^{-2}	4.34072×10^{-5}
		0.8	1.52842×10^{-2}	3.00619×10^{-5}
		0.9	1.51780×10^{-2}	2.59273×10^{-6}
		1.0	0.000000	0.000000

TABLE 5.2: Comparison of relative error between FDM and GOMM for moving front at $\alpha = 0$, $\delta = 0$, $\zeta = 0$ and $\nu = 1\ m^2 s^{-1}$ for different parameters.

S.No.	*Parameters*	*Time* τ/s	*Relative Error*$_{FDM}$	*Relative Error*$_{GOMM}$
1		1	1.03836×10^{-1}	2.96778×10^{-6}
		2	6.81695×10^{-2}	1.48389×10^{-6}
		3	5.32988×10^{-2}	1.33550×10^{-6}
		4	4.47807×10^{-2}	1.18711×10^{-6}
		5	3.91118×10^{-2}	1.03872×10^{-6}
	$Bi = 0.5$	6	3.50303×10^{-2}	8.90333×10^{-7}
	$Ste = 1.0$	7	3.19106×10^{-2}	7.41944×10^{-7}
		8	2.94479×10^{-2}	5.93555×10^{-7}
		9	2.74319×10^{-2}	4.45166×10^{-7}
		10	2.57493×10^{-2}	2.96778×10^{-7}
2		1	2.21878×10^{-1}	1.19408×10^{-6}
		2	1.57516×10^{-1}	3.52646×10^{-6}
		3	1.27809×10^{-1}	3.92424×10^{-6}
		4	1.09883×10^{-1}	3.24104×10^{-6}
	$Bi = 0.5$	5	9.75975×10^{-2}	3.24458×10^{-6}
	$Ste = 0.5$	6	8.85186×10^{-2}	3.00438×10^{-6}
		7	8.14654×10^{-2}	9.05068×10^{-6}
		8	7.57869×10^{-2}	7.05340×10^{-5}
		9	7.10910×10^{-2}	3.65669×10^{-6}
		10	6.7126×10^{-2}	6.82258×10^{-6}
3		1	8.36470×10^{-2}	2.33565×10^{-5}
		2	5.57874×10^{-2}	2.57735×10^{-5}
		3	4.37232×10^{-2}	2.53300×10^{-5}
		4	3.66994×10^{-2}	2.50656×10^{-5}
	$Bi = 1.0$	5	3.20051×10^{-2}	2.48852×10^{-5}
	$Ste = 0.5$	6	2.86030×10^{-2}	2.47520×10^{-5}
		7	2.60017×10^{-2}	2.46485×10^{-5}
		8	2.39353×10^{-2}	2.45650×10^{-5}
		9	2.22463×10^{-2}	2.44959×10^{-5}
		10	2.08348×10^{-2}	2.44374×10^{-5}

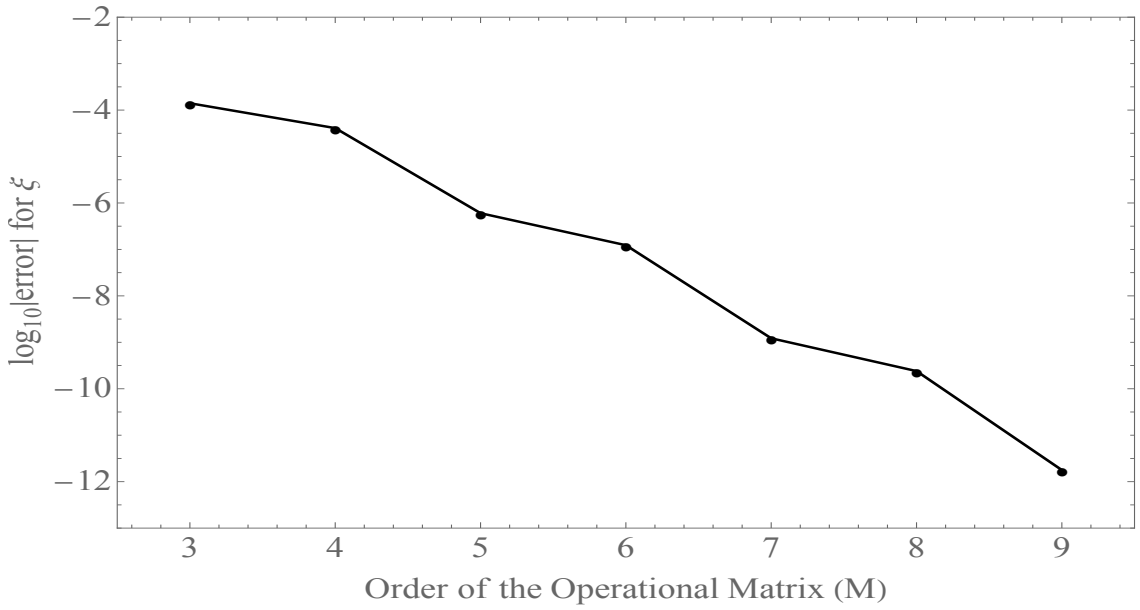

FIGURE 5.2: Convergence of approximation of ξ.

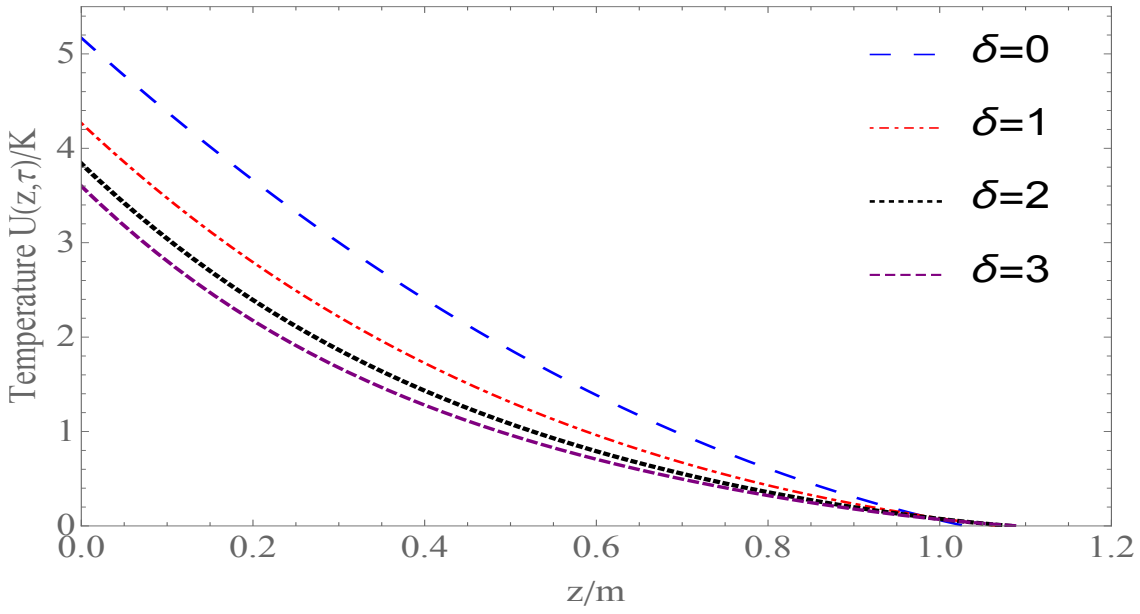

FIGURE 5.3: Effect of δ on temperature profile $(U(z,\tau))$ at $\tau = 5$.

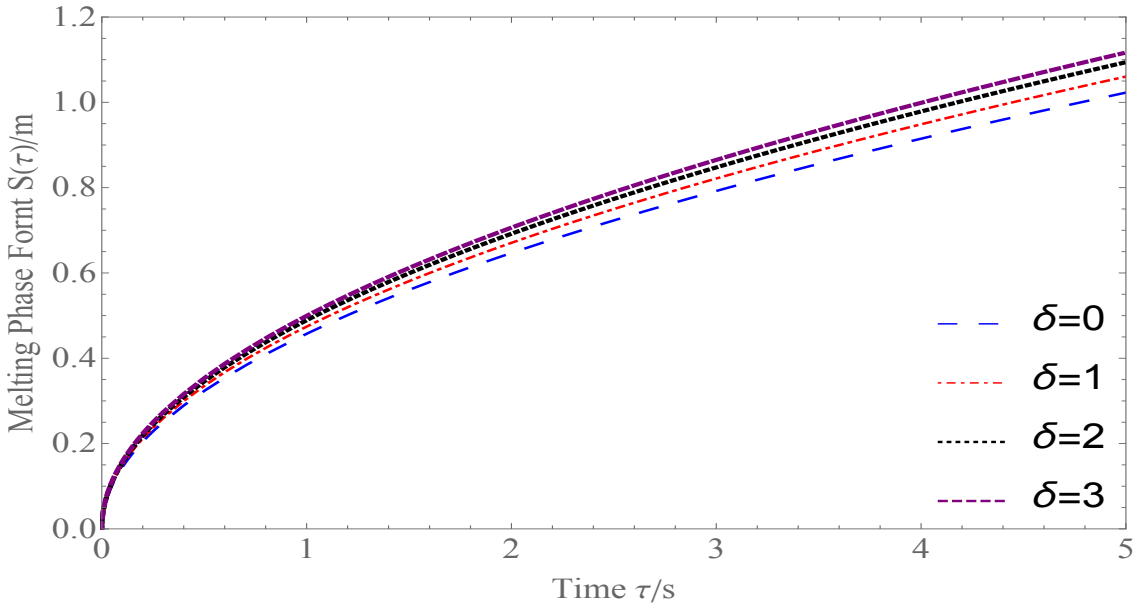

FIGURE 5.4: Effect of δ on moving phase front $S(\tau)$.

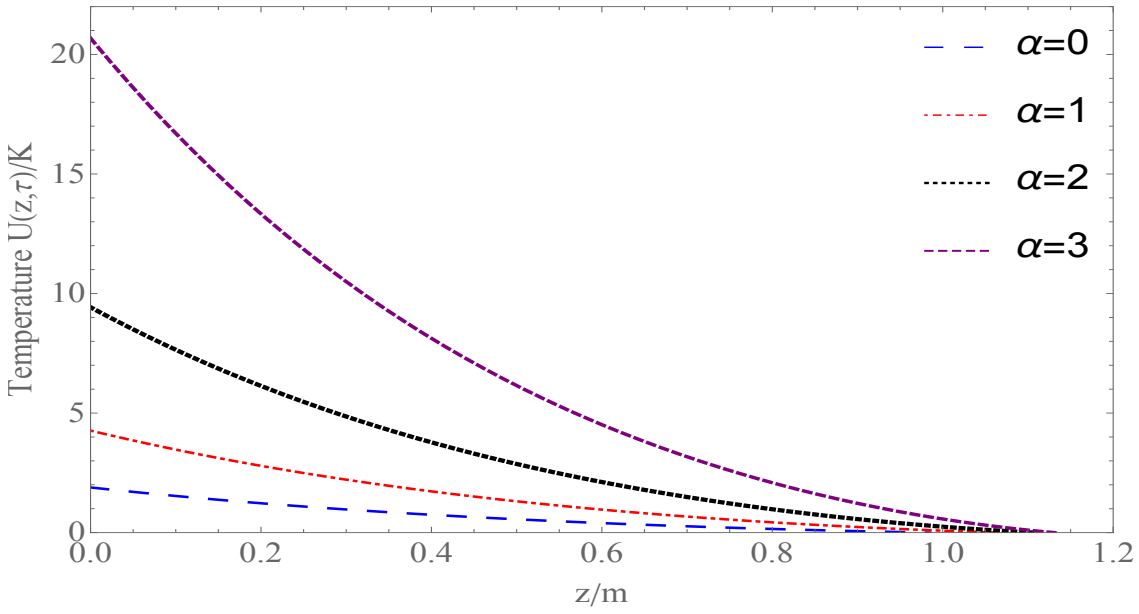

FIGURE 5.5: Effect of α on temperature profile $(U(z,\tau))$ at $\tau = 5$.

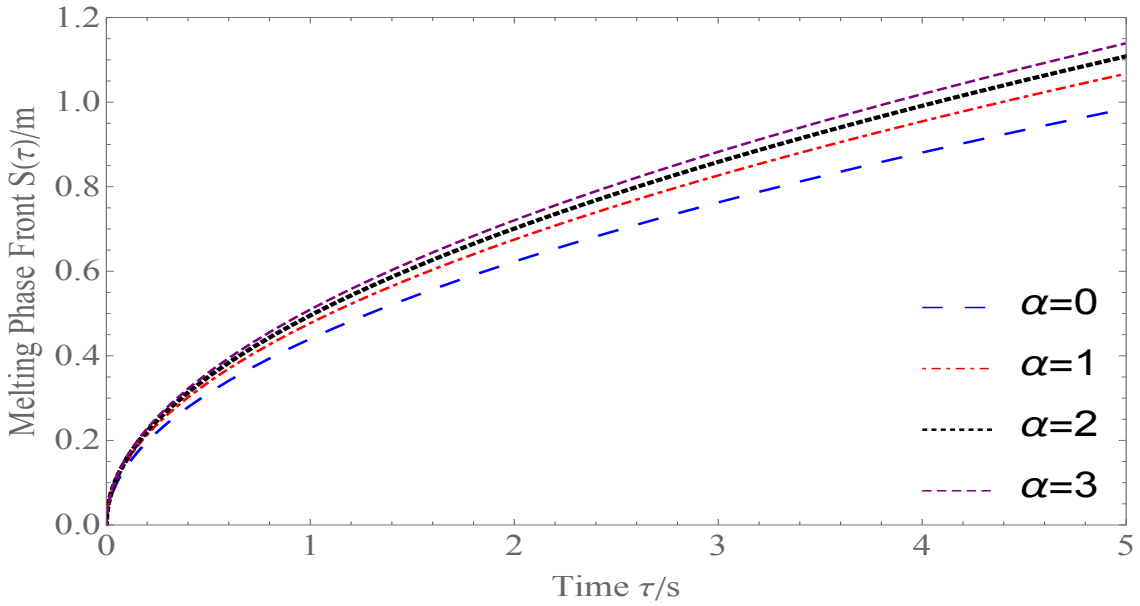

FIGURE 5.6: Effect of α on the evolution of moving phase front $S(\tau)$.

5.5 Conclusions

This chapter presents a mathematical model of a non-classical Stefan problem that includes the convective boundary condition, variable latent heat and space-dependent thermal conductivity. The collocation method with the aid of the operational matrix of Genocchi polynomials is applied to solve the proposed non-classical Stefan problem. For a particular case of the model, relative errors of the Genocchi operational matrix method (GOMM) and finite difference method (FDM) are shown in the tables. From the tables, it is found that the maximum percentage error of temperature for GOMM and FDM are 0.011902 % and 6.0833 %, respectively, which shows that the proposed GOMM is more accurate than the FDM for solving the Stefan problems. It is also observed that boundary fixation is the main fundamental problem when we use FDM to find the numerical solution of the Stefan problems. But, there is no need of boundary fixation in the case of GOMM,and this is an extra

advantage of GOMM over FDM. Moreover, the accuracy of the solution by GOMM for the Stefan problem improves as the order of the operational matrix or degree of Genocchi polynomials increases. Therefore, the proposed algorithm (GOMM) is a simple, reliable and accurate scheme to solve the non-classical Stefan problems. It is believed that the proposed approach will be a beneficial tool for the researchers working in this area. From this study, it is also observed that the parameters α and/or δ accelerate the speed of moving phase front. Hence, these parameters influence the phase change processes. Therefore, the manufacturers or researchers can control the phase change process by the parameters α and/or δ.

****